Laboratory Report of Digital Signal Processing

Name: Junjie Fang 123456

Student ID: 521260910018

Date: 2024/3/4

Score:

Contents

1 Continuous-Time Fourier Transform properties

1.a

The definition of *CTFT* is:

$$X_\omega = \int_{-\infty}^{+\infty} x(t) \cdot e^{-j\omega t} \, \mathrm{d}t$$

To integrate arbitrary functions in code, we use discrete sampling summation for approximate integration. The code is in Appendix 3.a. In this code, the `CTFT(x, t, w)` function take `x` and `t` as lists of sampled data in time domain, which should be calculated outside the function. For each element in `w`, which represents a frequency, the function calculates *CTFT* at this frequency, and finally return a list of complex numbers.

In order to improve the approximation accuracy, we can increase the number of samples (i.e. `SAMPLE_N` parameter).

1.b

We can get $g_2 = g\left(t - \frac{D}{2}\right)$ by applying time shifting on g. To get g_2 in the code, we use a function called `func_tranform` to get the shifted function of g. The figure showing both functions is:

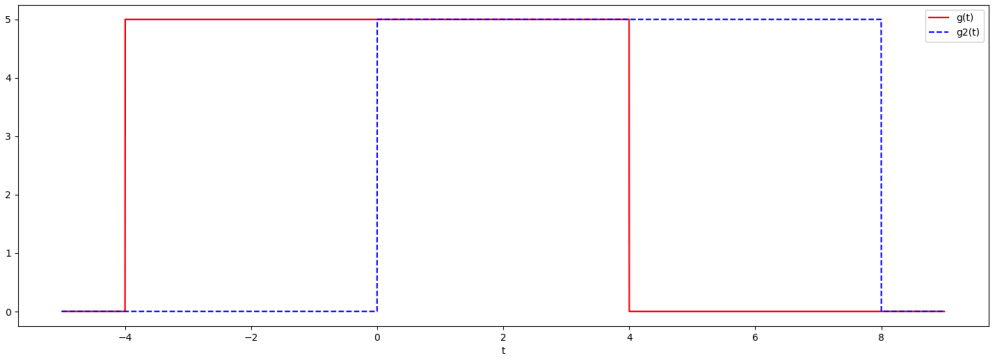

Figure 1: g and g_2 in the same plot

1.c

Using the function `CTFT()` function realized in *1.a*, we can calculate the *CTFT* of g_2 and g respectively.

By observing the images of module, phase, real part and imaginary part of the two functions, **we can verify the followling properties of time shifting under *CTFT*:**

1. The module remains unchanged.
2. THe phase changes linearly with ω, and the distribution of real and imaginary parts changes.

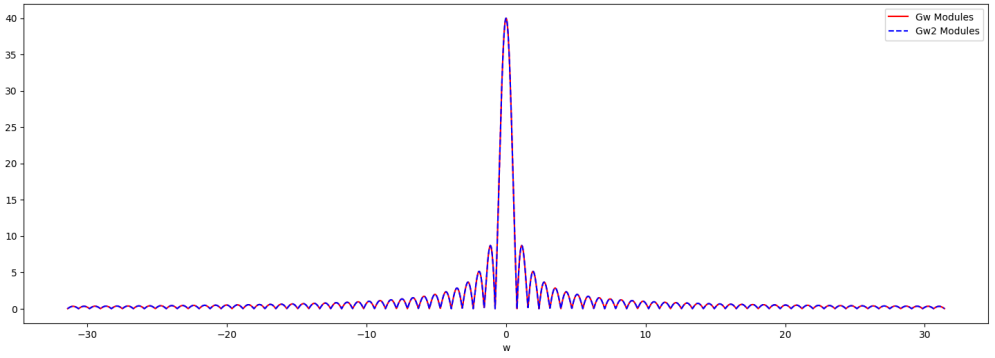

Figure 2: Module of g and g_2

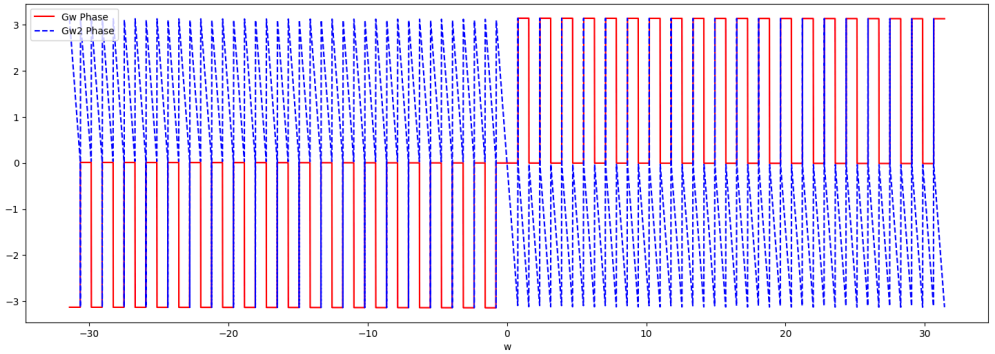

Figure 3: Phase of g and g_2

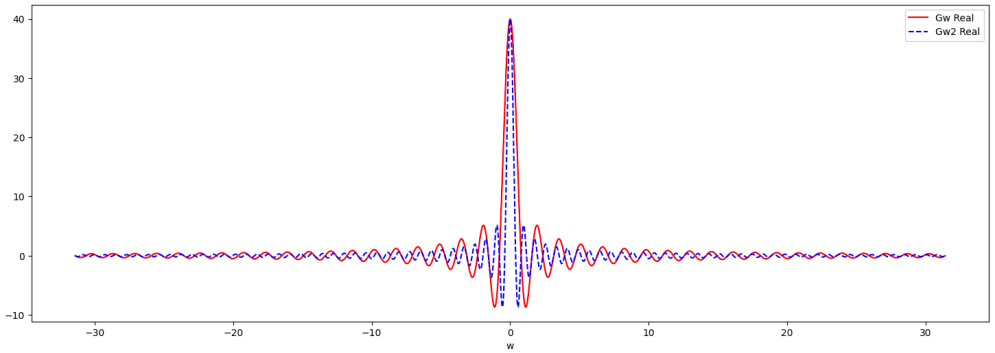

Figure 4: Real part of g and g_2

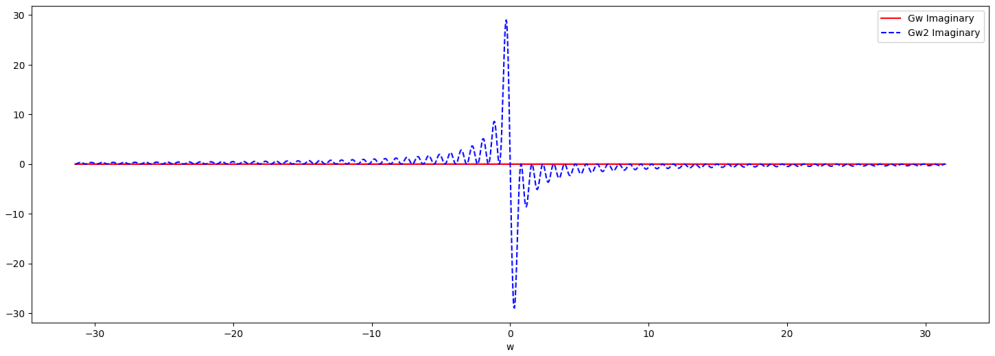

Figure 5: Imaginary part of g and g_2

1.d

In the code, we can generate $y(t) = g(t) \times \cos(4\pi t)$ from $g(t)$. The figure below shows the comparison of $g(t)$ and $y(t)$ over $t = [-15, 15]$:

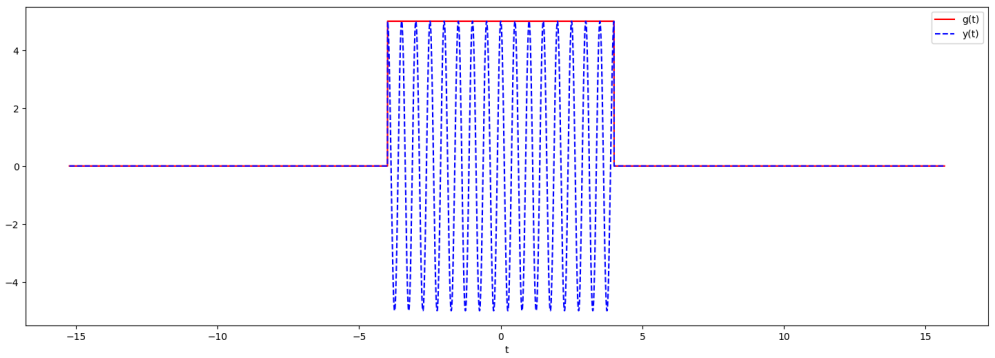

Figure 6: y and g in the same plot

1.e

To get the module and phase of $y(t)$ and $g(t)$, we can calculte their *CTFT* like in Section 1.c.

The modulation property of *CTFT* gives:

$$G_{T_1}(t)\cos(\omega_0 t) \overset{F.T.}{\Longleftrightarrow} \frac{1}{2}X[j(\omega-\omega_0)] + \frac{1}{2}X[j(\omega+\omega_0)]$$

This property can be verified from the figures below, as the module and phase of g is shifted to $\omega_0 = 4\pi$ and $-\omega_0 = -4\pi$ in the frequency domain. Note the peak value of module of y is half this value of g.

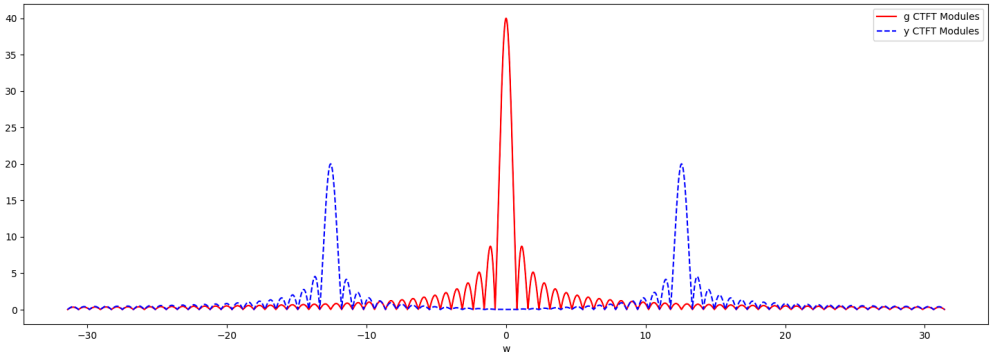

Figure 7: Module of y and g

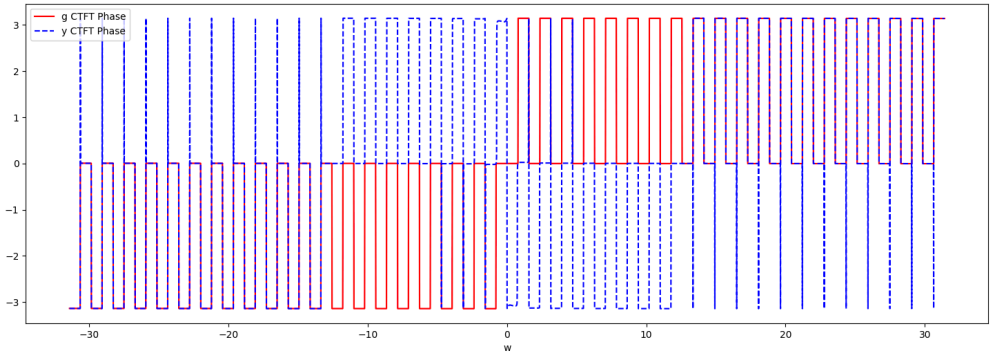

Figure 8: Phase of y and g

1.f

In the code we can get the energy in both time and frequency domain, which are 99.95 and 99.38. There is a slight difference, and we can consider the two energies to be the same. The difference comes from the error in the integral calculation and is very small (the error can be reduced by increasing the number of integral samples).

The reason behind that is Parseval's formula, which gives:

$$\int_{-\infty}^{+\infty} |x(t)|^2 \, \mathrm{d}t = \frac{1}{2\pi} \int_{-\infty}^{+\infty} |X(j\omega)|^2 \, \mathrm{d}\omega$$

This denotes that the energy in time domain is equal to the energy in frequency domain. The proof of this formula is as follows:

$$
\begin{aligned}
&\int_{-\infty}^{+\infty} x^2(t)\,\mathrm{d}t \\
&= \int_{-\infty}^{+\infty} x(t)\left(\frac{1}{2\pi}\int_{-\infty}^{+\infty} X(j\omega)e^{j\omega t}\,\mathrm{d}\omega\right)\mathrm{d}t \\
&= \frac{1}{2\pi}\int_{-\infty}^{+\infty} X(j\omega)\left(\int_{-\infty}^{+\infty} x(t)e^{j\omega t}\,\mathrm{d}t\right)\mathrm{d}\omega \\
&= \frac{1}{2\pi}\int_{-\infty}^{+\infty} X(j\omega)X(-j\omega)\,\mathrm{d}t \\
&= \frac{1}{2\pi}\int_{-\infty}^{+\infty} |X(j\omega)|^2\,\mathrm{d}t
\end{aligned}
$$

2 Discrete-Time Fourier Transform properties

2.a

The code in appendix implements `DTFT(nT, xn, w)` function, using the following formula:

$$X(\omega) = \sum_{n=-\infty}^{+\infty} x(nT)e^{-j\omega nT}$$

To avoid infinite calculation, we can set a start time and end time for sampling function, as long as it covers the whole signal.

2.b

Using the function implemented in *3.a*, we rendered the images of $G_{w,1}$ and $G_{w,2}$ in a Nyquist interval,

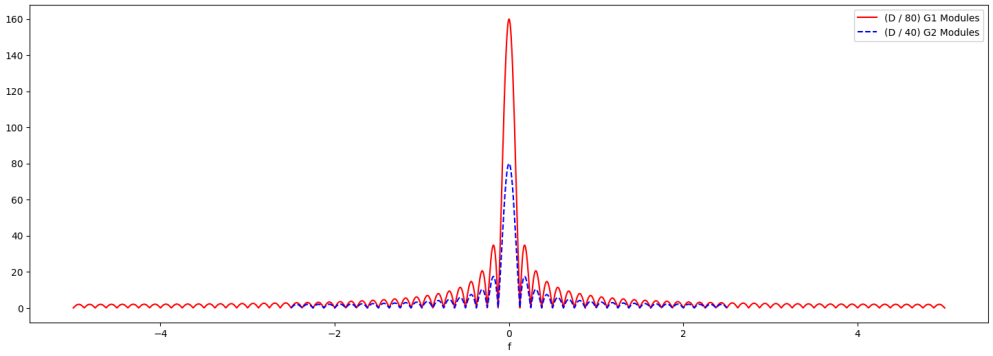

Figure 9: Module of $G_{w,1}$ and $G_{w,2}$ in f

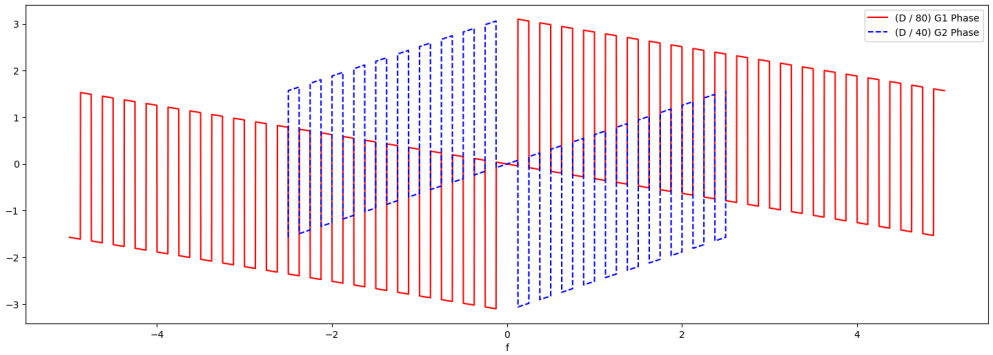

Figure 10: Phase of $G_{w,1}$ and $G_{w,2}$ in f

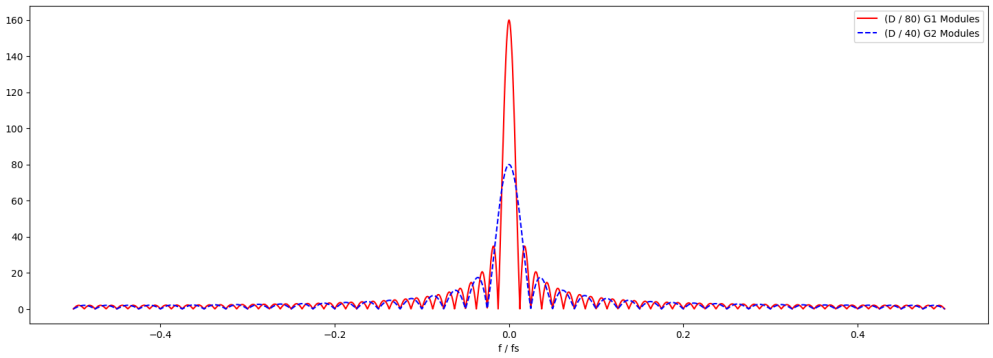

Figure 11: Module of $G_{w,1}$ and $G_{w,2}$ in $\frac{f}{f_s}$

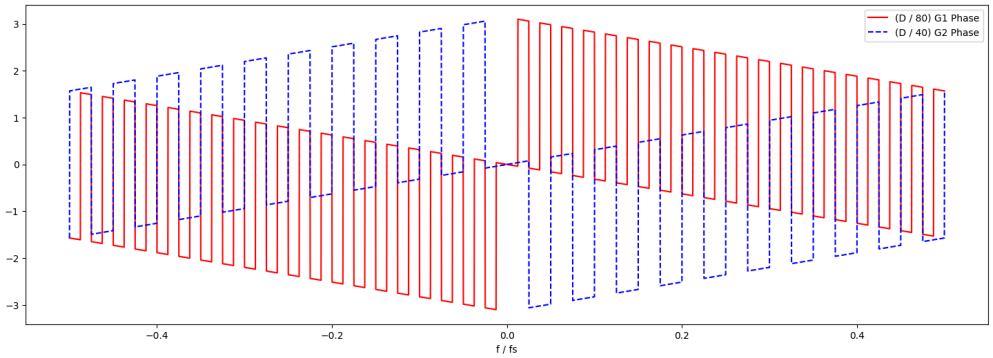

Figure 12: Phase of $G_{w,1}$ and $G_{w,2}$ in $\frac{f}{f_s}$

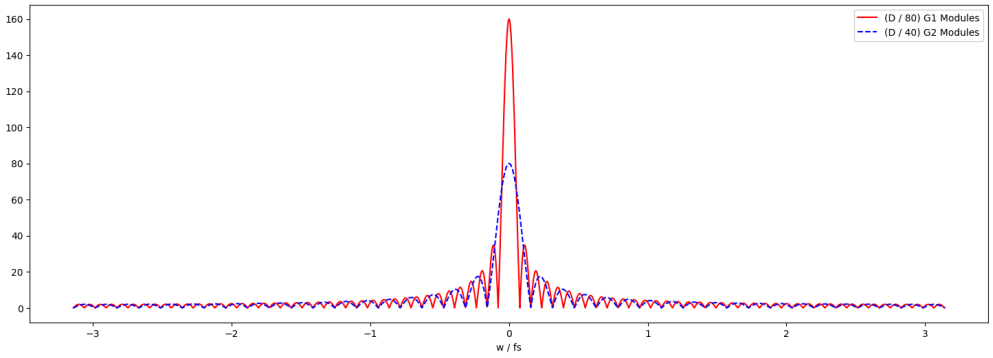

Figure 13: Module of $G_{w,1}$ and $G_{w,2}$ in $\frac{w}{f_s}$

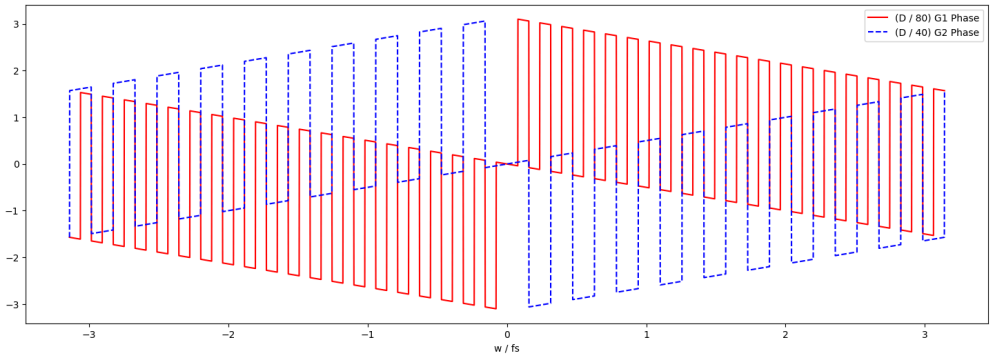

Figure 14: Phase of $G_{w,1}$ and $G_{w,2}$ in $\frac{w}{f_s}$

2.c

The theoretical *CTFT* function of g is:

$$\begin{aligned} X(w) &= \int_{-\infty}^{+\infty} g(t) e^{-j\omega t}\,\mathrm{d}t \\ &= \int_{-4}^{4} 2e^{-j\omega t}\,\mathrm{d}t \\ &= \frac{2}{-j\omega}(e^{-4j\omega} - e^{4j\omega}) \\ &= 16\,\mathrm{sinc}(4\omega) \end{aligned}$$

We can plot them in the same figure:

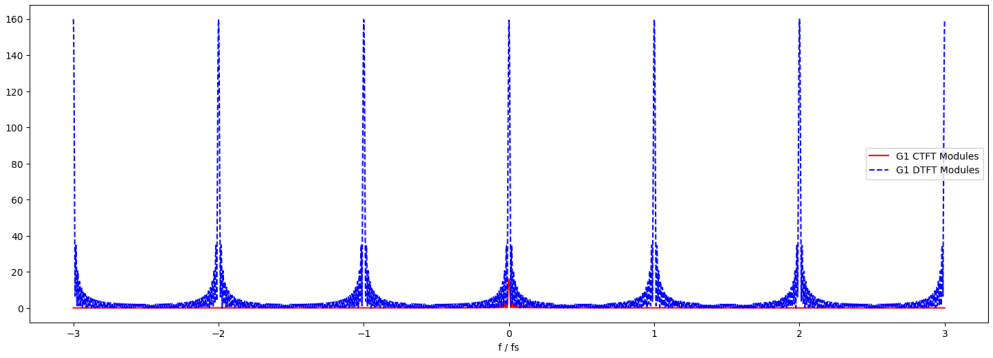

Figure 15: Module of $G_{w,1}$ and *CTFT* of g

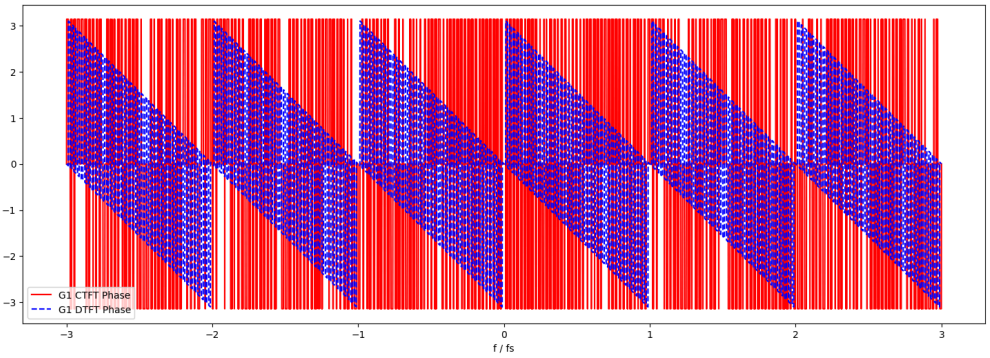

Figure 16: Phase of $G_{w,1}$ and *CTFT* of g

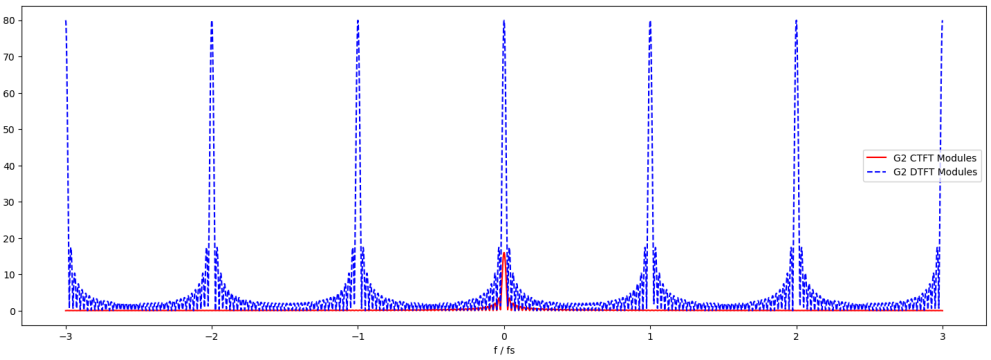

Figure 17: Module of $G_{w,2}$ and *CTFT* of g

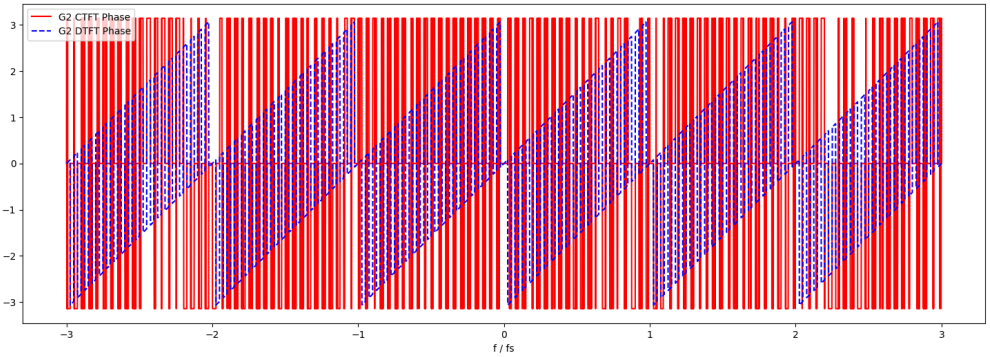

Figure 18: Phase of $G_{w,2}$ and *CTFT* of g

For $G_{w,1}$, the peak value at $\omega = 0$ is ten times the *CTFT* of g. That's because the sampling frequency is $f_s = 10$. And for $G_{w,2}$ it is five times, as the sampling frequency is $f_s = 5$.

2.d

We can inverse *DTFT* using the formula:

$$x[nT] = \frac{1}{w_s} \int_{-\frac{w_s}{2}}^{+\frac{w_s}{2}} X[e^{j\omega}] e^{j\omega n} \, \mathrm{d}\omega$$

We get:

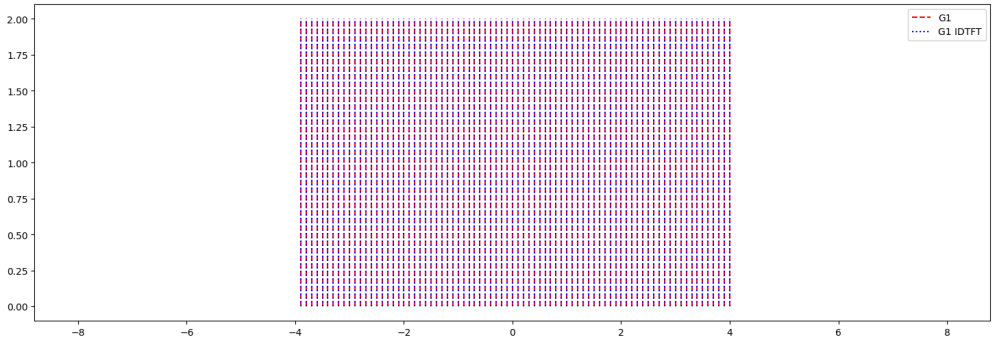

Figure 19: Figure of the discrete g_1 and the inverse of $G_{w,1}$

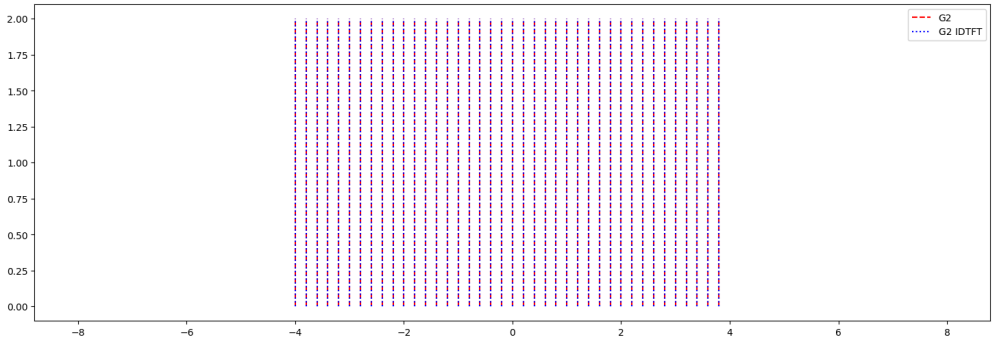

Figure 20: Figure of the discrete g_2 and the inverse of $G_{w,2}$

This two images shows that the inverse *DTFT* perfectly matches the discret sampling function.

2.e

The former Parseval's formula is no longer validated for *DTFT*. If we calculate the energy of the the original function and the *DTFT* function (in one Nyquist interval to avoid infinite energy), we can get 31.99 and 3199.99, the latter one is 100 times the former one. That is due to the sampling frequency of the discrete function.

We can adjust this result by adding a factor of $\left(\frac{1}{f_s}\right)^2$ in the formula of *DTFT* function, which means the Parseval's formula would be:

$$\int_{-\infty}^{+\infty} |x(t)|^2 \, \mathrm{d}t = \frac{1}{2\pi f_s^2} \int_{-\frac{w_s}{2}}^{+\frac{w_s}{2}} |X(j\omega)|^2 \, \mathrm{d}\omega$$

.

3 Windowing effects of DTFT

3.a

We can adopt $\frac{2}{N}$ as factor to scale magnitudes of *DTFT* function. The figure is:

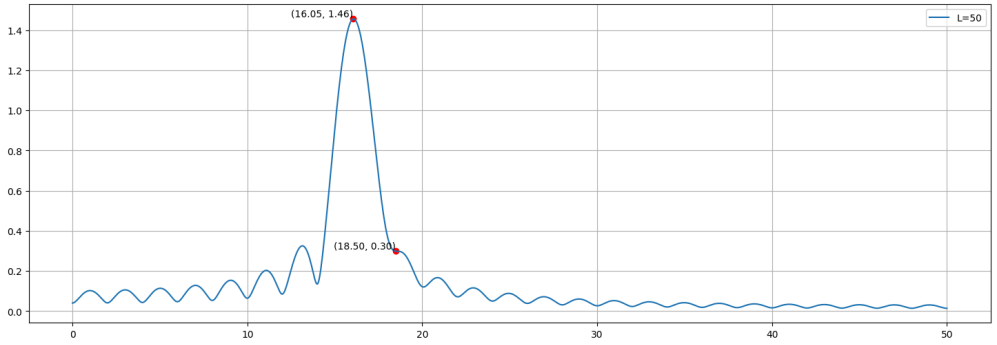

Figure 21: Figure and peak values when $L = 50$

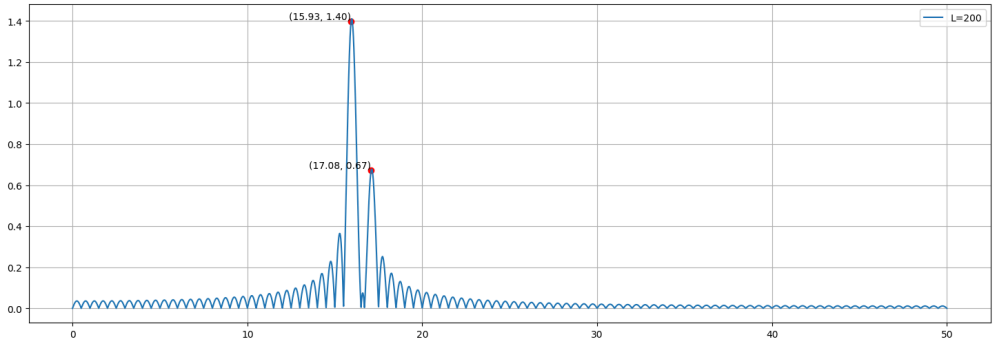

Figure 22: Figure and peak values when $L = 200$

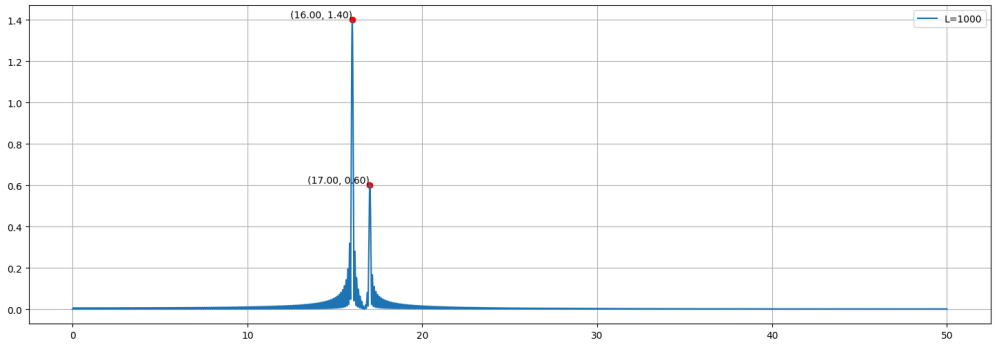

Figure 23: Figure and peak values when $L = 1000$

Larger the L, the more accurate we can find the right amplitude and frequency.

L	factor	A_1	A_2	f_1	f_2
50	$\frac{2}{50}$	1.46	0.30	16.05	18.50
200	$\frac{2}{200}$	1.40	0.67	15.93	17.08
1000	$\frac{2}{1000}$	1.40	0.60	16.00	17.00

3.b

Using hamming function, the factor should be $\frac{2a_0}{N}$, where $a_0 = 0.53836$. The figure is:

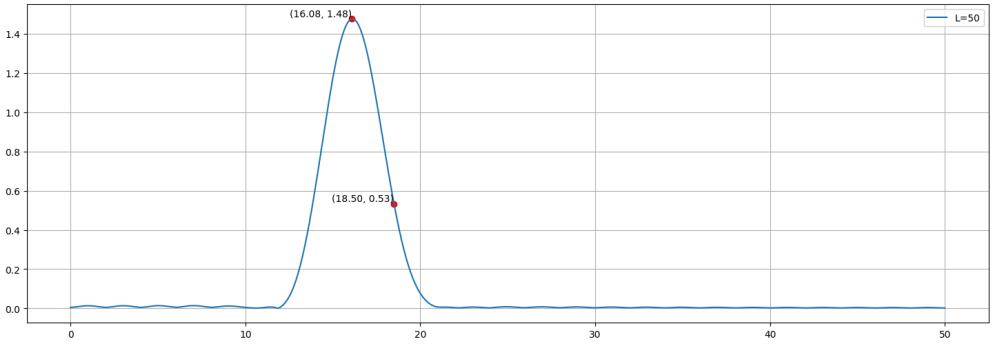

Figure 24: Figure and peak values when $L = 50$

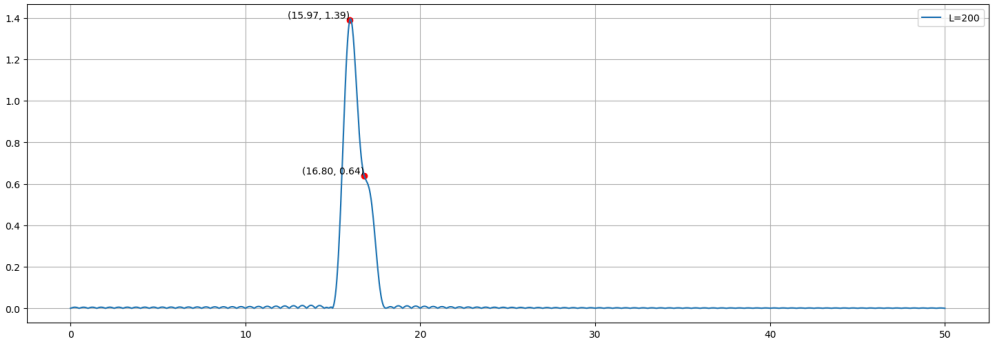

Figure 25: Figure and peak values when $L = 200$

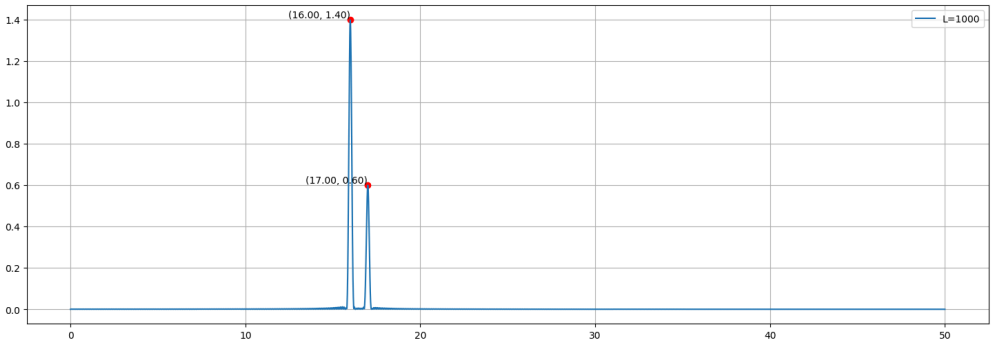

Figure 26: Figure and peak values when $L = 1000$

L	factor	A_1	A_2	f_1	f_2
50	$\frac{2a_0}{50}$	1.48	0.53	16.08	18.50
200	$\frac{2a_0}{200}$	1.39	0.64	15.97	16.80
1000	$\frac{2a_0}{1000}$	1.40	0.60	16.00	17.00

The sidelobes after applying hamming function are much lower than the original ones, which means the frequency leakage is reduced. But the width of the main lobe is increased, leading to a reduction of frequency resolution.